

Cluster Contrast for Unsupervised Person Re-Identification

Zuozhuo Dai^{1*} Guangyuan Wang^{1*} Weihao Yuan¹ Xiaoli Liu¹ Siyu Zhu¹ Ping Tan^{1,2}
¹Alibaba A.I. Labs ²Simon Fraser University

Abstract

State-of-the-art unsupervised re-ID methods train the neural networks using a memory-based non-parametric softmax loss. Instance feature vectors stored in memory are assigned pseudo-labels by clustering and updated at instance level. However, the varying cluster sizes leads to inconsistency in the updating progress of each cluster. To solve this problem, we present Cluster Contrast which stores feature vectors and computes contrast loss at the cluster level. Our approach employs a unique cluster representation to describe each cluster, resulting in a cluster-level memory dictionary. In this way, the consistency of clustering can be effectively maintained throughout the pipeline and the GPU memory consumption can be significantly reduced. Thus, our method can solve the problem of cluster inconsistency and be applicable to larger data sets. In addition, we adopt different clustering algorithms to demonstrate the robustness and generalization of our framework. The application of Cluster Contrast to a standard unsupervised re-ID pipeline achieves considerable improvements of 9.9%, 8.3%, 12.1% compared to state-of-the-art purely unsupervised re-ID methods and 5.5%, 4.8%, 4.4% mAP compared to the state-of-the-art unsupervised domain adaptation re-ID methods on the Market, Duke, and MSMT17 datasets. Code is available at <https://github.com/alibaba/cluster-contrast>.

1. Introduction

Deep unsupervised person Re-identification (re-ID) aims to train a neural network capable of retrieving a person of interest across cameras without any labeled data. This task has attracted increasing attention recently due to the growing demands in practical video surveillance and the expensive labeling cost. There are mainly two approaches to address this problem. One is the purely un-supervised learning (USL) person re-ID, which generally exploits pseudo labels from the completely unlabeled data [9, 10, 12, 24, 41]. The other is the unsupervised domain adaptation (UDA) person re-ID, which first pre-trains a model on the source labeled dataset, and then fine-tunes the model on the target unlabeled dataset [7, 23, 42, 44, 49, 55, 56]. Generally, the performance of UDA is superior to that of USL because of the introduction of the external source domain. However, UDA still suffers from the complex training procedure and

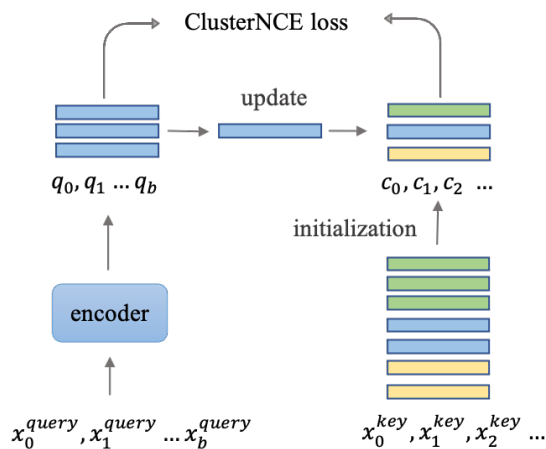


Figure 1. The Cluster Contrast computes the contrastive loss in cluster level. In the cluster level memory dictionary, the cluster feature is initialized through uniformly sample a random instance feature from the corresponding cluster and updated by the batch query instance. $x \in X$ is the training dataset. q is the query instance feature vector. c_k stands for the k -th cluster feature vector. Feature vectors with the same color belong to the same cluster.

requires that the difference between the source and target domain is not significant.

In this paper, we focus on learning the person re-ID task without any labeled data (i.e., USL). Existing state-of-the-art USL methods [12, 41] exploit memory dictionary and pseudo labels from clustering to train the neural network. At the beginning of each epoch, all the image features of the training data are extracted by the current neural network. We regard these image features stored in memory as the dictionary. Then, a clustering algorithm, like DBSCAN [8] or K-means [29] is employed to cluster image features and produce pseudo labels. Meanwhile, the cluster ID is assigned to each image as the person identity. Finally, the neural network is trained with a contrastive loss such as triplet loss [18, 35], InfoNCE loss [30], or other non-parametric classification loss [41] based on the memory dictionary. Although these pseudo-label-based methods achieve good performance, there is still a large gap between USL and supervised methods, which limits USL in practical applications.

To bridge the gap, we re-investigate the pseudo-label-based USL pipeline and argue that the memory dictionary

storage mechanism, including the initialization, updating, and loss computation, is crucial for model optimization. The state-of-the-art approaches store the feature vector of every instance inside the memory dictionary and computes the multi-label non-parametric classification loss [41] or InfoNCE loss [30] with the query instance. Such memory dictionary storage mechanism have two main drawbacks. First, the feature updating progress of memory dictionary is inconsistent, since the distribution of training data is biased in the instance level. This problem is especially serious in large-scale re-ID datasets like MSMT17 [44]. Second, the cluster centroid is not an optimal feature representation of pseudo-labels in memory dictionary. Since the clustering approach inevitably introduces noisy labels, such an averaging operation of features within a cluster [12] would contaminate its corresponding cluster feature representation as well.

To solve these two problems, we propose the Cluster Contrast. It builds a cluster-level memory dictionary in which each cluster is represented by a single feature vector and all cluster feature vectors are consequently updated in a consistent manner. More specifically, this cluster feature is initialized as the average feature of all images from the cluster and momentum updated by the batch query instance feature during training. Accordingly, we propose a cluster-level InfoNCE loss, denoted as ClusterNCE loss, which computes contrastive loss between cluster feature and query instance feature as illustrated in Figure 1. Based on the cluster-level memory dictionary, the ClusterNCE loss takes much less GPU memory than the instance-level feature memory, and consequently allows our method to be trained on a larger dataset.

In summary, our proposed Cluster Contrast USL has several advantages, which are as follows:

- We introduce the cluster contrast which initializes, updates, and performs contrastive loss computation at cluster level. It uses a unique cluster representation to solve the cluster consistency problem. To our knowledge, this is the first work to maintain the clustering consistency across the whole pipeline.
- Our approach adopts a simple pipeline, which is significantly different from existing approaches. All cluster representations can be stored and updated by building a cluster-level memory dictionary. This simple strategy enables us to take up less GPU memory, which allows our method to be trained on larger data sets.
- Our method provides a general framework for effective utilization of different clustering algorithms. We employ DBSCAN and InfoMap in our framework, both of which have been proven to be effective on different magnitudes of data sets.

- We demonstrate that the proposed unsupervised approach with Cluster Contrast surpasses all the existing unsupervised person re-ID methods by a significant margin.

2. Related Work

Deep Unsupervised Person Re-ID. Deep unsupervised person re-ID can be summarized into two categories. The first category is unsupervised domain adaptation (UDA) re-ID, which utilizes transfer learning to improve unsupervised person re-ID [7, 23, 42, 44, 49, 55, 56]. The second category is pure unsupervised learning (USL) person re-ID [9, 10, 12, 24, 41], which trains model directory on unlabeled dataset. State-of-the-art USL re-ID pipeline generally involves three stages: memory dictionary initialization, pseudo label generation, and neural network training. Previous works have made significant improvements either in parts or on the whole pipeline. Specifically, Lin et al. [24] treats each individual sample as a cluster, and then gradually groups similar samples into one cluster to generate pseudo labels. MMCL [41] predicts quality pseudo labels comprising of similarity computation and cycle consistency. It then trains the model as a multi-classification problem. SPCL [12] proposes a novel self-paced contrastive learning framework that gradually creates more reliable cluster to refine the memory dictionary features. In this paper, we propose the Cluster Contrast to improve the memory dictionary and loss function part. Next we discuss related studies with respect to these two aspects.

Memory Dictionary. Contrast learning [14] can be thought of as training an encoder for a dictionary look-up task. Several recent studies [2, 15, 17, 19, 30, 38, 46, 58] on unsupervised visual representation learning present promising results through building dynamic dictionaries. The memory dictionary is updated consistently on the fly to facilitate contrastive unsupervised learning. Similar to unsupervised visual representation learning, state-of-the-art unsupervised person re-ID methods also build memory dictionaries for contrastive learning [11, 12, 41, 47]. During training, instance feature vectors in the memory dictionary are updated by the corresponding query instances features.

Loss Functions. In supervised person re-ID, the batch hard triplet loss has proved to be effective solutions to improve the re-ID performance [3–5, 13, 26, 36, 40, 52, 57]. In unsupervised person re-ID, since there is no ground truth person identity and the pseudo labels are changing during training, non-parametric classification loss such as InfoNCE [30] are used as identity loss. Similar to InfoNCE, Tong et al. [47] designs an Online Instance Matching (OIM) loss with a memory dictionary scheme which compares query image to a memorized feature set

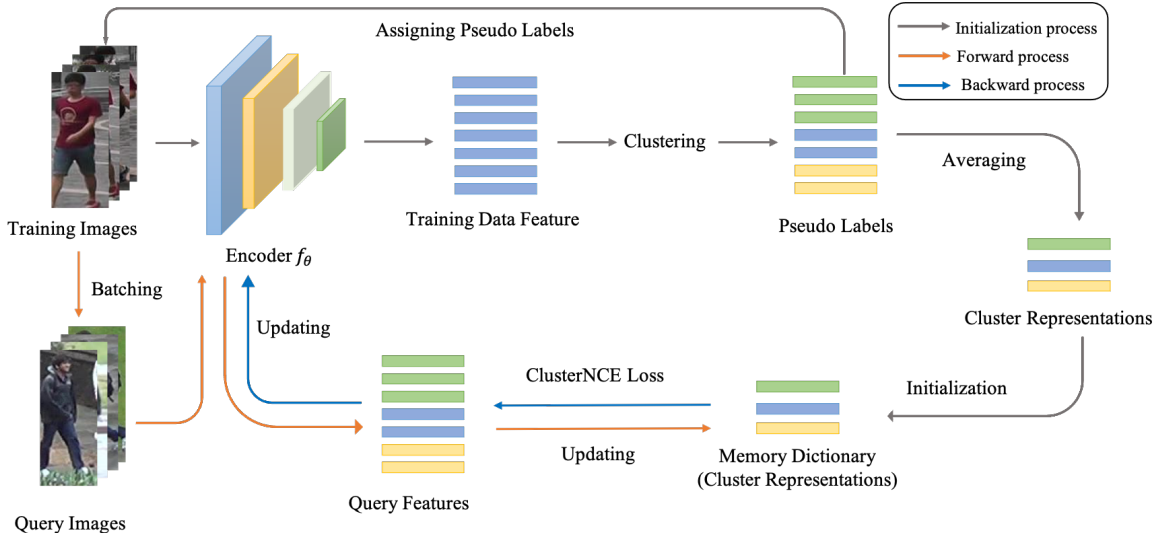


Figure 2. The system pipeline of our unsupervised person re-ID method. The upper branch depicts the memory initialization stage. The training data features are assigned pseudo labels by clustering, where features of the same color belong to the same cluster. The lower branch represents the model training stage. Query features in iterative mini-batch are used to update the memory cluster representations with a momentum. The ClusterNCE loss computes the contrastive loss between query features and all cluster representations.

of unlabelled identities. Wang and Zhang [41] introduce the memory-based non-parametric multi-label classification loss (MMCL), which treat USL re-ID as a multi-label classification problem. In order to mitigate noisy pseudo labels, MMT [11] proposes a novel soft softmax-triplet loss to support learning with soft pseudo triplet labels. SPCL [12] introduces a unified contrastive loss including both source domain dataset and target domain dataset. In this paper, we apply InfoNCE loss between cluster feature and query instance feature on USL re-ID.

3. Proposed Method

We first introduce our overall approach at a high level in Section 3.1. Then, we compare the different contrast learning methods with our clustering contrast learning method in Section 3.2. Finally in Section 3.3, we explain the details of cluster contrast along with the working theory.

3.1. USL Person Re-ID via Cluster Contrast

State-of-the-art USL methods [11, 12, 41] solve the USL Person Re-ID problem with contrastive learning. Specifically, they build a memory dictionary that contains the features of all training images. Each feature is assigned a pseudo ID generated by a clustering algorithm. During training, the contrastive loss is minimized to train the network to learn a proper feature embedding that is consistent with the pseudo ID.

We focused on designing a proper contrast function to keep the whole pipeline simple while obtaining better performance. An overview of our training pipeline is shown in

Figure 2. The memory dictionary initialization is illustrated in the upper branch. We use a standard ResNet50 [16] as the backbone encoder which is pretrained on ImageNet to extract feature vectors, and has basic discriminability though not optimized for re-ID tasks. We then apply the DBSCAN [8] and InfoMap [34] clustering algorithms to cluster similar features together and assign pseudo labels to them. The pseudo labels are further refined by cycle consistency, where two images are assigned with the same label if they share similar neighbors. We then calculate the mean feature vectors of each cluster to form a set of cluster representations. The memory dictionary is initialized by these cluster representations and their corresponding pseudo labels. As shown in the lower branch, during the training stage, we compute the ClusterNCE loss between the query image features and all cluster representations in the dictionary to train the network. Meanwhile, the dictionary features are updated with a momentum by the query features.

3.2. Contrastive Learning

To facilitate the description of methods, we first introduce the notations used in this paper. Let $X = \{x_1, x_2, \dots, x_N\}$ denote the training set with N instances. And $U = \{u_1, u_2, \dots, u_n\}$ denotes the corresponding features obtained from the backbone encoder f_θ , described as $u_i = f_\theta(x_i)$. q is a query instance feature extracted by $f_\theta(\cdot)$, where the query instance belongs to X . In this section, we analyze different contrastive learning methods to motivate our cluster contrastive consistency learning.

As shown in Figure 3 (a), the multi-label classification loss computes the loss in the instance level through

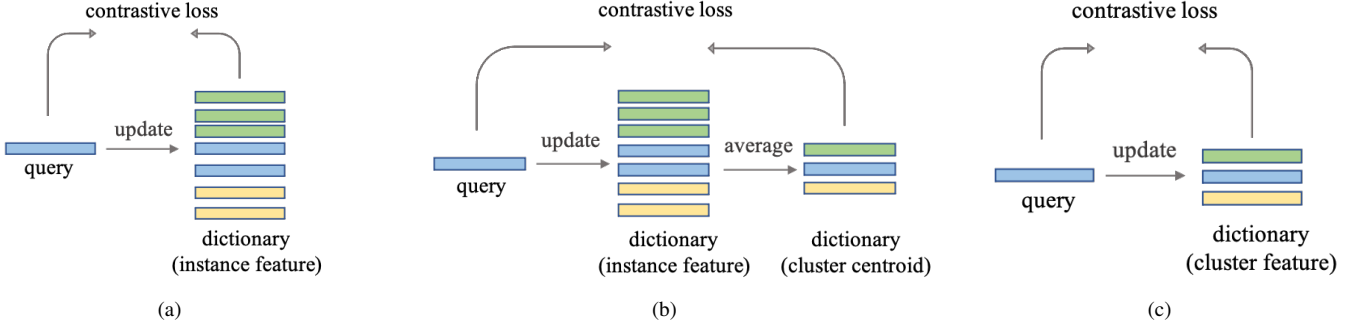


Figure 3. Comparison of three types of memory-based nonparametric contrastive learning losses. Different color features indicate different clusters. (a) Multi-label classification loss. It computes the loss and updates the memory dictionary both at the instance level. (b) Instance level InfoNCE loss. It computes the loss at the cluster level but updates the memory dictionary at the instance level. (c) ClusterNCE loss. It computes the loss and updates the memory dictionary both at the cluster level.

an instance-wise contrastive loss, defined by InfoNCE loss [15] as follows:

$$L_q = -\log \frac{\exp(q \cdot u_+/\tau)}{\sum_{i=0}^N \exp(q \cdot u_i/\tau)} \quad (1)$$

where τ is a temperature hyper-parameter. The memory dictionary is updated at the instance level as:

$$u_i \leftarrow m u_i + (1 - m) q \quad (2)$$

where m is the momentum updating factor. It stores all image feature vectors and computes multi-class score by comparing query feature q to all image feature vectors in the memory dictionary. The memory dictionary is updated by the q after each training iteration.

In Figure 3 (b), SPCL [12] computes the loss at cluster level through a cluster-wise contrastive loss. It can be defined as follows:

$$L_q = -\log \frac{\exp(q \cdot c_+/\tau)}{\sum_{k=0}^K \exp(q \cdot c_k/\tau)} \quad (3)$$

where $\{c_1, c_2, \dots, c_K\}$ is the cluster centroids and K stands for the number of clusters. It uses the cluster centroid as the cluster level feature vector to compute the distances between query instance and all the clusters. The cluster centroids are calculated by the mean feature vectors of each cluster as:

$$c_k = \frac{1}{|\mathcal{H}_k|} \sum_{u_i \in \mathcal{H}_k} u_i \quad (4)$$

where \mathcal{H}_k denotes the k -th cluster set and $|\cdot|$ indicates the number of instances per cluster. \mathcal{H}_k contains all the feature vectors in the cluster k . But similar to multi-classification loss, it stores all image feature vectors in the memory dictionary. The stored image feature vectors are then updated by corresponding query image feature using Eq. 2.

Both Figure 3 (a) and Figure 3 (b) update the feature vectors at an instance level by using Eq. 2, resulting in cluster

inconsistency problem. As shown in Figure 4, the cluster size is unbalancedly distributed. In every training iteration, in a large cluster only a small fraction of the instance features can be updated, whereas in a small cluster all the instances can be updated. Thus, the updating process is highly varied, leading to biased clustering centers. Some clustering centers are determined by the updated instances, while others rely on the unupdated instances. In each iteration, the network is constantly updated, which causes inconsistent oscillatory distribution of mini-batches. In contrast, we design our ClusterNCE loss as shown in Figure 3 (c) using the following equation:

$$L_q = -\log \frac{\exp(q \cdot \phi_+/\tau)}{\sum_{k=0}^K \exp(q \cdot \phi_k/\tau)} \quad (5)$$

where ϕ_k is the unique representation vector of the k -th cluster. It updates the feature vectors and computes the loss both in the cluster level. It's worth noting that the memory dictionary stores all cluster feature representations and can be updated consistently as:

$$\phi_k \leftarrow m \phi_k + (1 - m) q \quad (6)$$

We can see that, our proposed algorithm uses unique feature vectors to represent each cluster category and remains distinct throughout the updating process, which is the most significant difference from the previous contrastive loss approaches. In the next section, we will discuss in detail how our method consistently updates the cluster representation to maintain the cluster consistency.

3.3. Cluster Contrast Learning

The proposed Cluster Contrast involves the process of memory dictionary initialization, memory updating, and neural network training. The training details are presented in Algorithm 1.

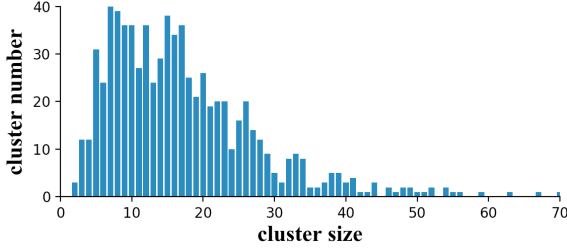


Figure 4. The cluster size follows a normal distribution in Market1501 dataset.

Memory Initialization. Different from the instance level memory dictionary, we store each cluster’s representation $\{\phi_1, \dots, \phi_K\}$ in the memory-based feature dictionary. We use the mean feature vectors of each cluster to initialize the cluster representation, that is

$$\phi_k = \frac{1}{|\mathcal{H}_k|} \sum_{u_i \in \mathcal{H}_k} u_i \quad (7)$$

Eq. 7 is executed when each epoch is initialized. And the clustering algorithm runs in each epoch, so K is changing as the model trains.

Memory Updating. During training, P person identities and a fixed number Z of instances for each person identity were sampled from the training set. Consequently, we obtain a total number of $P \times Z$ query images in the mini batch [18]. We use the Eq. 6 to momentum update the cluster representation as illustrated in Figure 3. It is worth noting that all cluster representations are stored in the memory dictionary, so we calculate loss by comparing each query instance with all cluster representations in each iteration. In contrast to the previous instance-level feature memory methods [11, 12], the $P \times Z$ query instance features were just updated in the instance level memory through Eq. 2. By substituting Eq. 2 into Eq. 4, the clustering centroids of SPCL after each iteration can be obtained by

$$c_k \leftarrow \frac{1}{|\mathcal{H}_k|} \left\{ \sum_{\substack{u_i \in \mathcal{H}_k \\ u_i \in \mathcal{Q}}} [mu_i + (1 - m)q] + \sum_{\substack{u_i \in \mathcal{H}_k \\ u_i \notin \mathcal{Q}}} u_i \right\} \quad (8)$$

where \mathcal{Q} denotes the query instance features set, which contains all the feature vectors of query images for one iteration. From Eq. 8, it can be clearly seen that each iteration only updates part of the instances in each cluster, which belong to \mathcal{Q} , but the instances in the cluster which are not in \mathcal{Q} are not updated. After an epoch, all mini-batch instances are updated iteratively, that is, all instances are updated once. This can be expressed as \mathcal{Q} contains all the instances in the cluster, i.e $\mathcal{Q} \supseteq \mathcal{H}_k$, such that $\sum_{u_i \in \mathcal{H}_k, u_i \notin \mathcal{Q}} u_i = 0$. Then Eq. 8 can be written as:

$$\begin{aligned} c_k &\leftarrow \frac{1}{|\mathcal{H}_k|} \sum_{\substack{u_i \in \mathcal{H}_k \\ u_i \in \mathcal{Q}}} [mu_i + (1 - m)q] \\ &= m \frac{1}{|\mathcal{H}_k|} \sum_{\substack{u_i \in \mathcal{H}_k \\ u_i \in \mathcal{Q}}} u_i + (1 - m) \frac{1}{|\mathcal{H}_k|} \sum_{\substack{u_i \in \mathcal{H}_k \\ u_i \in \mathcal{Q}}} q \quad (9) \\ &= mc_k + (1 - m)q \end{aligned}$$

Most notably, the cluster center can be updated consistently once only if one epoch is completed. However, our update method, Eq. 6, maintains the consistent representation of clustering throughout the training process. By comparing the above equations, it can be seen that our method updates the clustering representation uniquely, which can solve the consistency problem.

Loss Function. We use Eq. 5 to calculate the cluster feature loss. The loss value is low when q is similar to its positive cluster feature ϕ_+ and dissimilar to all other cluster representations. It is a log loss of K -way softmax-based classifier that tries to classify q as ϕ_+ .

Algorithm 1: USL pipeline with Cluster Contrast

Require: Unlabeled training data X

Require: Initialize the backbone encoder f_θ with ImageNet-pretrained ResNet-50

Require: Temperature τ for Eq. 5

Require: Momentum m for Eq. 6

for n in $[1, num_epochs]$ **do**

 Extract feature vectors U from X by f_θ

 Clustering U into K clusters with DBSCAN or InfoMap

 Initialize memory dictionary with Eq. 7

for i in $[1, num_iterations]$ **do**

 Sample $P \times K$ query images from X

 Compute ClusterNCE loss with Eq. 5

 Update cluster feature with Eq. 6

end

end

4. Experiment

4.1. Datasets and Implementation

Datasets We evaluate our proposed method on four large-scale person re-identification (re-ID) benchmarks: Market-1501 [53], DukeMTMC-reID [33], MSMT17 [44], PersonX [37], and one vehicle ReID dataset, VeRi-776 [27]. The Market-1501, DukeMTMC-reID, and MSMT17 are widely used real-world person re-identification tasks. The PersonX is synthesized based on Unity [32], which contains manually designed obstacles such as random occlusion, resolution, and lighting differences. To show the robustness of

Dataset	Object	#train IDs	#train images	#test IDs	#query images	#total images	#cameras
MSMT17	Person	1,041	32,621	3,060	11,659	126,441	15
PersonX	Person	410	9,840	856	5,136	45,792	6
Market-1501	Person	751	1 2,936	750	3,368	32,668	6
DukeMTMC-reID	Person	702	16,522	702	2,228	36,441	8
VeRi-776	Vehicle	575	37,746	200	1,678	51,003	20

Table 1. Statistics of datasets used in the experimental section.

Methods	Market-1501				
	source	mAP	top-1	top-5	top-10
BUC [24]	None	38.3	66.2	79.6	84.5
SSL [25]	None	37.8	71.7	83.8	87.4
MMCL [41]	None	45.5	80.3	89.4	92.3
MMCL [41]	Duke	60.4	84.4	92.8	95.0
HCT [50]	None	56.4	80.0	91.6	95.2
CycAs [43]	None	64.8	84.8	-	-
AD-Cluster++ [51]	Duke	68.3	86.7	94.4	96.5
UGA [45]	None	70.3	87.2	-	-
MMT [11]	MSMT17	75.6	89.3	95.8	97.5
SPCL [12]	MSMT17	77.5	89.7	96.1	97.6
SPCL/Infomap	None	70.7	86.3	93.6	95.6
SPCL [12]	None	73.1	88.1	95.1	97.0
Ours/Dbscan	None	82.1	92.3	96.7	97.9
Ours/Infomap	None	83.0	92.9	97.2	98.0

(a) Experiments on Market-1501 datasets

Methods	DukeMTMC-reID				
	source	mAP	top-1	top-5	top-10
BUC [24]	None	27.5	47.4	62.6	68.4
SSL [25]	None	28.6	52.5	63.5	68.9
MMCL [48]	None	51.4	72.4	82.9	85.0
AD-Cluster++ [51]	Market	54.1	72.6	82.5	85.5
MMCL [41]	Market	51.4	72.4	82.9	85.0
HCT [50]	None	50.7	69.6	83.4	87.4
UGA [45]	None	53.3	75.0	-	-
CycAs [43]	None	60.1	77.9	-	-
MMT [11]	Market	65.1	78.9	88.8	92.5
SPCL [12]	Market	68.8	82.9	90.1	92.5
SPCL/Infomap	None	61.8	79.5	86.8	89.6
SPCL [12]	None	65.3	81.2	90.3	92.2
Ours/Dbscan	None	72.6	84.9	91.9	93.9
Ours/Infomap	None	73.6	85.5	92.2	94.3

(b) Experiments on DukeMTMC-reID datasets

Methods	MSMT17				
	source	mAP	top-1	top-5	top-10
ECN [56]	Duke	10.2	30.2	41.5	46.8
MMCL [48]	None	11.2	35.4	44.8	49.8
TAUDL [21]	None	12.5	28.4	-	-
UTAL [22]	None	13.1	31.4	-	-
UGA [45]	None	21.7	49.5	-	-
MMT [11]	Market	24.0	50.1	63.5	69.3
CycAs [43]	None	26.7	50.1	-	-
SPCL [12]	Market	26.8	53.7	65.0	69.8
SPCL/Infomap	None	17.2	40.6	53.6	59.2
SPCL [12]	None	19.1	42.3	55.6	61.2
Ours/Dbscan	None	27.6	56.0	66.8	71.5
Ours/Infomap	None	31.2	61.5	71.8	76.7

(c) Experiments on MSMT17 datasets

Methods	PersonX				
	source	mAP	top-1	top-5	top-10
MMT [11]	Market	78.9	90.6	96.8	98.2
SPCL [12]	Market	78.5	91.1	97.8	99.0
SPCL/Infomap	None	70.5	86.1	94.6	96.3
SPCL [12]	None	72.3	88.1	96.6	98.3
Ours/Dbscan	None	84.7	94.4	98.3	99.3
Ours/Infomap	None	86.6	95.3	98.8	99.5

(d) Experiments on PersonX datasets

Methods	VeRi-776				
	source	mAP	top-1	top-5	top-10
MMT [11]	VehicleID	35.3	74.6	82.6	87.0
SPCL [12]	VehicleID	38.9	80.4	86.8	89.6
SPCL/Infomap	None	34.7	73.9	81.8	86.9
SPCL [12]	None	36.9	79.9	86.8	89.9
Ours/Dbscan	None	40.3	84.6	89.2	91.6
Ours/Infomap	None	40.8	86.2	90.5	92.8

(e) Experiments on VeRi-776 datasets

Table 2. Comparison with state-of-the-art methods on the object re-ID, including unsupervised methods and unsupervised domain adaptation methods. “None” represents the pure unsupervised method. Other value represents the source-domain dataset in unsupervised domain adaptation method. “SPCL/Infomap” represents the result of SPCL retraining through the Infomap clustering method.

our method, we also conduct vehicle re-identification experiments on the widely used real scene VeRi-776 datasets. The details of these datasets are summarized in Table 1.

Implementation Details We adopt ResNet-50 [16] as the backbone encoder of the feature extractor and initialize the model with the parameters pre-trained on ImageNet [6]. After layer-4, we remove all sub-module layers and add global

average pooling (GAP) followed by batch normalization layer [20] and L2-normalization layer, which will produce 2048-dimensional features. During testing, we take the features of the global average pooling layer to calculate the distance. At the beginning of each epoch, we use DBSCAN [8] and InfoMap [34] for clustering to generate pseudo labels, respectively.

Method	Datase	ResNet-50		IBN-ResNet-50	
		mAP	top-1	mAP	top-1
Dbscan	Market-1501	81.8	92.5	83.3	92.6
	DukeMTMC-reID	72.6	84.9	74.7	86.0
	MSMT17	27.6	56.0	36.2	66.6
	PersonX	84.7	94.4	87.0	94.4
	VeRi-776	40.3	84.6	41.5	86.3
Informap	Market-1501	83.0	92.9	83.5	93.1
	DukeMTMC-reID	73.6	85.5	75.1	86.2
	MSMT17	31.2	61.5	40.6	70.1
	PersonX	86.6	95.3	89.2	96.0
	VeRi-776	40.8	86.2	42.2	89.2

Table 3. Comparison with IBN-ResNet-50 and ResNet-50 backbones in our method.

The input image is resized 256 x 128 for Market-1501, PersonX and MSMT17 datasets, and 224 x 224 for VeRi-776. For training images, we perform random horizontal flipping, padding with 10 pixels, random cropping, and random erasing [54]. Each mini-batch contains 256 images of 16 pseudo person identities (16 instances for each person). We adopt Adam optimizer to train the re-ID model with weight decay 5e-4. The initial learning rate is set to 3.5e-4, and is reduced to 1/10 of its previous value every 20 epoch in a total of 50 epoch. To demonstrate the generalization ability of our method, we apply both the DBSCAN and InfoMap [1] clustering method for pseudo-label assignment. For DBSCAN, we used the same parameter settings as [12] where the maximum distance d between two samples is 0.6 and the minimal number of neighbors in a core point is 4. For InfoMap, we adopt two-level and directed links network for clustering where no hyper-parameter required to set.

4.2. Comparison with State-of-the-arts

Compared with SOTA USL Methods. We first compare our method to State-of-the-arts USL methods which is the main focus of our method. From Table 2, we can see that our method is significantly better than all existing unsupervised methods, which proves the effectiveness of our method. Based on the same pipeline and DBSCAN clustering method, the mAP of our method surpasses the state-of-the-art USL method SPCL [12] by 9.0%, 8.5%, 7.3%, 12.4% and 3.4% on Market-1501 [53], MSMT17 [44], DukeMTMC-reID [33], PersonX [37], and VeRi-776 [27] respectively.

Compared with SOTA UDA Methods. We also compare our method with State-of-the-arts UDA re-ID methods. The UDA methods can make full use of the labeled source domain datasets, so they usually achieve better results than the USL re-ID methods. The ClusterNCE loss could also be easily generalized to UDA re-ID methods. Table 2 shows that the mAP of our pure unsupervised re-ID method still outperforms the SOTA UDA method [12] by up to 6% even

Batch size	Baseline		Ours	
	mAP	Rank-1	mAP	Rank-1
32	62.5	80.3	75.9	89.5
64	65.5	82.7	80.2	91.2
128	71.5	86.7	81.8	92.0
256	73.1	87.3	82.1	92.3

Table 4. The impact of batch size to baseline method and our method on Market1501 dataset.

Cluster Size	#Instance	Fraction	mAP	Rank-1
20	4	0.2	67.6	84.4
8	4	0.5	71.4	85.9
5	4	0.8	73.2	87.5
4	4	1.0	76.5	89.0

Table 5. The impact of cluster size to baseline method on Market1501 dataset.

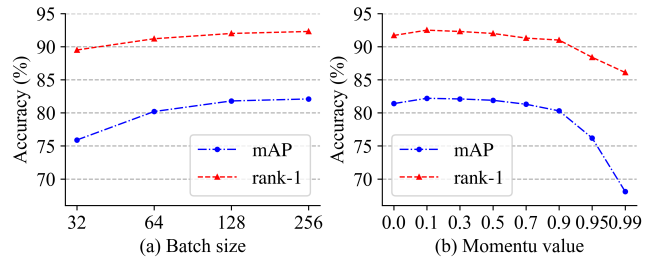


Figure 5. The impact of (a) batch size and (b) momentum value on Market-1501 datasets.

though they use more training data.

Compared with Different Clustering Algorithms As shown in Table 2, in addition to the DBSCAN clustering algorithm which is widely used in previous re-ID methods, the Cluster Contrast can achieve better results with the InfoMap clustering algorithm. Infomap is a network clustering algorithm based on the Map Equation [34] which aims to minimize the information needed to move between different clusters. It has fewer hyper-parameters than DBSCAN.

Compared with IBN-ResNet-50 and ResNet-50 backbones. Instance-batch normalization (IBN) [31] combines the advantages of IN [39] learning appearance invariance features and BN [20] learning content-related information. It has been proved effective in object re-ID methods in supervised [28] learning tasks. As shown in Table 3, using IBN-ResNet as backbone can further improve performance.

4.3. Ablation Studies

In this section, we study the effectiveness of various components in Cluster Contrast method. We define the USL pipeline with instance-level memory dictionary (Figure 3 (b)) as the **baseline** method.

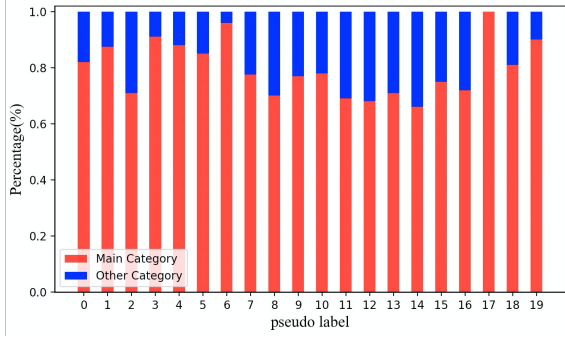


Figure 6. We randomly select 20 categories from the Market1501 clustering results and calculate the percentage of different categories using ground truth labels.

Memory Updating Consistency In section 3.3, we argue that compared to instance-level memory, the cluster-level memory could update cluster feature more consistently. As shown in Figure 3 (b), the instance-level memory dictionary maintains the feature of each instance of the dataset. In every training iteration, each instance feature in the mini-batch will be updated to its own memory dictionary. Since the cluster size is unbalancedly distributed, only a small fraction of the instance features could be updated in a large cluster when all instances in a small cluster are updated.

The simplest solution is to increase the batch size. As the batch size increases, more instance features could be updated inside one cluster. As shown in Table 4, the performance of the baseline increases as the batch size increases. However, the batch size reaches its upper limit of 256 due to the GPU memory.

To deal with the limitation of the GPU memory, we came up another solution that we restrict the cluster size to a constant number. Therefore, in every iteration a fixed fraction of the instance features could be updated. In this way, the instance feature vectors can be updated consistently with a small batch size. The results in Table 5 demonstrate that the performance of the baseline increases with the rising of the fraction of the updated instance features, until all instance feature vectors inside one cluster could be updated in a single iteration. In sum, we propose the Cluster Contrast, which can update the cluster feature representation in single iteration.

Cluster Feature Representation As shown in Figure 3 (b), the instance-level memory averages all instance feature vectors to represent the cluster feature. However, in USL re-ID, the pseudo label generation stage would inevitably introduce the outlier instances. In Figure 6, we count the proportions of different real categories being clustered into the same category on the Market-1501 dataset. It shows there still around 20% noisy instances when model training is finished. These incorrect instance feature vectors

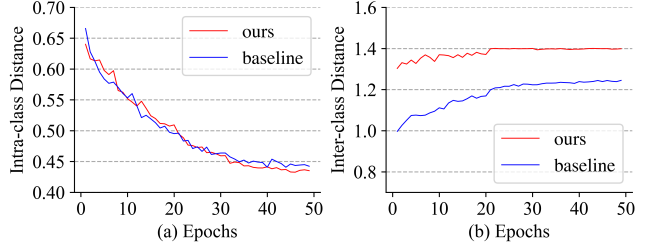


Figure 7. Comparison of intra-class distance and inter-class distance between our method and baseline method on Market1501 datasets.

are averaged along with correct instance feature vectors to compute the cluster feature centroid, which is harmful to the cluster representation. Our method can get better feature representation as shown in Figure 7. The feature quality of our method measured by the intra-class distance and the inter-class distance are much better than the baseline method. From this we can speculate that better representation of features between classes is an important factor for our method to achieve better results.

Momentum Values. We use the momentum update strategy to update cluster representations in memory dictionary. As shown in Eq. 6, the momentum value m controls the update speed of cluster memory. The larger the value of m , the slower the cluster memory update. We conducted experiments on the Market-1501 dataset to explore the influence of different m values on our method. As shown in Figure 5 (b), it performs reasonably well when m is less than 0.9. When m is too large (e.g., greater than 0.9), the accuracy drops considerably. These results support us to build better cluster representation.

Batch Size. To explore the impact of different batch sizes on our method, we use different batch sizes from 32 to 256 to train our method. From the experimental results shown in Figure 5 (a), we can see that a large batch size will achieve better results. Comparing to the baseline method in Table 4, the performance of our method remains stable over a wide range of batch sizes from 64 to 256.

5. Conclusion

In this paper, we present the Cluster Contrast mechanism, which stores feature vectors and computes contrast loss in cluster level memory dictionary. It unifies the cluster feature updating progress regardless the cluster size or dataset size. And it uses a more robust cluster feature representation to compute the contrastive loss. Experiments show that the simple USL pipeline with Cluster Contrast surpassing all existing USL and UDA re-ID methods.

References

- [1] <https://www.mapequation.org/infomap/>. 7
- [2] Philip Bachman, R Devon Hjelm, and William Buchwalter. Learning representations by maximizing mutual information across views. *arXiv preprint arXiv:1906.00910*, 2019. 2
- [3] Guangyi Chen, Chunze Lin, Liangliang Ren, Jiwen Lu, and Jie Zhou. Self-critical attention learning for person re-identification. In *Proceedings of the IEEE/CVF International Conference on Computer Vision*, pages 9637–9646, 2019. 2
- [4] Zuozhuo Dai, Mingqiang Chen, Xiaodong Gu, Siyu Zhu, and Ping Tan. Batch dropblock network for person re-identification and beyond. In *Proceedings of the IEEE/CVF International Conference on Computer Vision*, pages 3691–3701, 2019. 2
- [5] Zuozhuo Dai, Mingqiang Chen, Siyu Zhu, and Ping Tan. Batch feature erasing for person re-identification and beyond. *arXiv preprint arXiv:1811.07130*, 1(2):3, 2018. 2
- [6] Jia Deng, Wei Dong, Richard Socher, Li-Jia Li, Kai Li, and Li Fei-Fei. Imagenet: A large-scale hierarchical image database. In *2009 IEEE conference on computer vision and pattern recognition*, pages 248–255. Ieee, 2009. 6
- [7] Weijian Deng, Liang Zheng, Qixiang Ye, Guoliang Kang, Yi Yang, and Jianbin Jiao. Image-image domain adaptation with preserved self-similarity and domain-dissimilarity for person re-identification. In *Proceedings of the IEEE conference on computer vision and pattern recognition*, pages 994–1003, 2018. 1, 2
- [8] Martin Ester, Hans-Peter Kriegel, Jörg Sander, Xiaowei Xu, et al. A density-based algorithm for discovering clusters in large spatial databases with noise. In *Kdd*, volume 96, pages 226–231, 1996. 1, 3, 6
- [9] Hehe Fan, Liang Zheng, Chenggang Yan, and Yi Yang. Unsupervised person re-identification: Clustering and fine-tuning. *ACM Transactions on Multimedia Computing, Communications, and Applications (TOMM)*, 14(4):1–18, 2018. 1, 2
- [10] Yang Fu, Yunchao Wei, Guanshuo Wang, Yuqian Zhou, Honghui Shi, and Thomas S Huang. Self-similarity grouping: A simple unsupervised cross domain adaptation approach for person re-identification. In *Proceedings of the IEEE/CVF International Conference on Computer Vision*, pages 6112–6121, 2019. 1, 2
- [11] Yixiao Ge, Dapeng Chen, and Hongsheng Li. Mutual mean-teaching: Pseudo label refinery for unsupervised domain adaptation on person re-identification. *arXiv preprint arXiv:2001.01526*, 2020. 2, 3, 5, 6
- [12] Yixiao Ge, Feng Zhu, Dapeng Chen, Rui Zhao, and hongsheng Li. Self-paced contrastive learning with hybrid memory for domain adaptive object re-id. In H. Larochelle, M. Ranzato, R. Hadsell, M. F. Balcan, and H. Lin, editors, *Advances in Neural Information Processing Systems*, volume 33, pages 11309–11321. Curran Associates, Inc., 2020. 1, 2, 3, 4, 5, 6, 7
- [13] Jianyuan Guo, Yuhui Yuan, Lang Huang, Chao Zhang, Jin-Ge Yao, and Kai Han. Beyond human parts: Dual part-aligned representations for person re-identification. In *Proceedings of the IEEE/CVF International Conference on Computer Vision*, pages 3642–3651, 2019. 2
- [14] Raia Hadsell, Sumit Chopra, and Yann LeCun. Dimensionality reduction by learning an invariant mapping. In *2006 IEEE Computer Society Conference on Computer Vision and Pattern Recognition (CVPR'06)*, volume 2, pages 1735–1742. IEEE, 2006. 2
- [15] Kaiming He, Haoqi Fan, Yuxin Wu, Saining Xie, and Ross Girshick. Momentum contrast for unsupervised visual representation learning. In *Proceedings of the IEEE/CVF Conference on Computer Vision and Pattern Recognition*, pages 9729–9738, 2020. 2, 4
- [16] Kaiming He, Xiangyu Zhang, Shaoqing Ren, and Jian Sun. Deep residual learning for image recognition. In *Proceedings of the IEEE conference on computer vision and pattern recognition*, pages 770–778, 2016. 3, 6
- [17] Olivier Henaff. Data-efficient image recognition with contrastive predictive coding. In *International Conference on Machine Learning*, pages 4182–4192. PMLR, 2020. 2
- [18] Alexander Hermans, Lucas Beyer, and Bastian Leibe. In defense of the triplet loss for person re-identification. *arXiv preprint arXiv:1703.07737*, 2017. 1, 5
- [19] R Devon Hjelm, Alex Fedorov, Samuel Lavoie-Marchildon, Karan Grewal, Phil Bachman, Adam Trischler, and Yoshua Bengio. Learning deep representations by mutual information estimation and maximization. *arXiv preprint arXiv:1808.06670*, 2018. 2
- [20] Sergey Ioffe and Christian Szegedy. Batch normalization: Accelerating deep network training by reducing internal covariate shift. In *International conference on machine learning*, pages 448–456. PMLR, 2015. 6, 7
- [21] Minxian Li, Xiatian Zhu, and Shaogang Gong. Unsupervised person re-identification by deep learning tracklet association. In *Proceedings of the European conference on computer vision (ECCV)*, pages 737–753, 2018. 6
- [22] Minxian Li, Xiatian Zhu, and Shaogang Gong. Unsupervised tracklet person re-identification. *IEEE transactions on pattern analysis and machine intelligence*, 42(7):1770–1782, 2019. 6
- [23] Shan Lin, Haoliang Li, Chang-Tsun Li, and Alex Chichung Kot. Multi-task mid-level feature alignment network for unsupervised cross-dataset person re-identification. *arXiv preprint arXiv:1807.01440*, 2018. 1, 2
- [24] Yutian Lin, Xuanyi Dong, Liang Zheng, Yan Yan, and Yi Yang. A bottom-up clustering approach to unsupervised person re-identification. In *Proceedings of the AAAI Conference on Artificial Intelligence*, volume 33, pages 8738–8745, 2019. 1, 2, 6
- [25] Yutian Lin, Lingxi Xie, Yu Wu, Chenggang Yan, and Qi Tian. Unsupervised person re-identification via softened similarity learning. In *Proceedings of the IEEE/CVF Conference on Computer Vision and Pattern Recognition*, pages 3390–3399, 2020. 6
- [26] Jinxian Liu, Bingbing Ni, Yichao Yan, Peng Zhou, Shuo Cheng, and Jianguo Hu. Pose transferrable person re-identification. In *Proceedings of the IEEE Conference on Computer Vision and Pattern Recognition*, pages 4099–4108, 2018. 2

- [27] Xinchen Liu, Wu Liu, Huadong Ma, and Huiyuan Fu. Large-scale vehicle re-identification in urban surveillance videos. In *2016 IEEE International Conference on Multimedia and Expo (ICME)*, pages 1–6. IEEE, 2016. 5, 7
- [28] Hao Luo, Youzhi Gu, Xingyu Liao, Shenqi Lai, and Wei Jiang. Bag of tricks and a strong baseline for deep person re-identification. In *Proceedings of the IEEE/CVF Conference on Computer Vision and Pattern Recognition Workshops*, pages 0–0, 2019. 7
- [29] James MacQueen et al. Some methods for classification and analysis of multivariate observations. In *Proceedings of the fifth Berkeley symposium on mathematical statistics and probability*, volume 1, pages 281–297. Oakland, CA, USA, 1967. 1
- [30] Aaron van den Oord, Yazhe Li, and Oriol Vinyals. Representation learning with contrastive predictive coding. *arXiv preprint arXiv:1807.03748*, 2018. 1, 2
- [31] Xingang Pan, Ping Luo, Jianping Shi, and Xiaoou Tang. Two at once: Enhancing learning and generalization capacities via ibn-net. In *Proceedings of the European Conference on Computer Vision (ECCV)*, pages 464–479, 2018. 7
- [32] John Riccitiello. John riccitiello sets out to identify the engine of growth for unity technologies (interview). *VentureBeat. Interview with Dean Takahashi*. Retrieved January, 18(3), 2015. 5
- [33] Ergys Ristani, Francesco Solera, Roger Zou, Rita Cucchiara, and Carlo Tomasi. Performance measures and a data set for multi-target, multi-camera tracking. In *European conference on computer vision*, pages 17–35. Springer, 2016. 5, 7
- [34] Martin Rosvall and Carl T Bergstrom. Maps of random walks on complex networks reveal community structure. *Proceedings of the national academy of sciences*, 105(4):1118–1123, 2008. 3, 6, 7
- [35] Florian Schroff, Dmitry Kalenichenko, and James Philbin. Facenet: A unified embedding for face recognition and clustering. In *Proceedings of the IEEE conference on computer vision and pattern recognition*, pages 815–823, 2015. 1
- [36] Jifei Song, Yongxin Yang, Yi-Zhe Song, Tao Xiang, and Timothy M Hospedales. Generalizable person re-identification by domain-invariant mapping network. In *Proceedings of the IEEE/CVF Conference on Computer Vision and Pattern Recognition*, pages 719–728, 2019. 2
- [37] Xiaoxiao Sun and Liang Zheng. Dissecting person re-identification from the viewpoint of viewpoint. In *Proceedings of the IEEE/CVF Conference on Computer Vision and Pattern Recognition*, pages 608–617, 2019. 5, 7
- [38] Yonglong Tian, Dilip Krishnan, and Phillip Isola. Contrastive multiview coding. *arXiv preprint arXiv:1906.05849*, 2019. 2
- [39] Dmitry Ulyanov, Andrea Vedaldi, and Victor Lempitsky. Improved texture networks: Maximizing quality and diversity in feed-forward stylization and texture synthesis. In *Proceedings of the IEEE Conference on Computer Vision and Pattern Recognition*, pages 6924–6932, 2017. 7
- [40] Cheng Wang, Qian Zhang, Chang Huang, Wenyu Liu, and Xinggong Wang. Mancs: A multi-task attentional network with curriculum sampling for person re-identification. In *Proceedings of the European Conference on Computer Vision (ECCV)*, pages 365–381, 2018. 2
- [41] Dongkai Wang and Shiliang Zhang. Unsupervised person re-identification via multi-label classification. In *Proceedings of the IEEE/CVF Conference on Computer Vision and Pattern Recognition*, pages 10981–10990, 2020. 1, 2, 3, 6
- [42] Jingya Wang, Xiatian Zhu, Shaogang Gong, and Wei Li. Transferable joint attribute-identity deep learning for unsupervised person re-identification. In *Proceedings of the IEEE Conference on Computer Vision and Pattern Recognition*, pages 2275–2284, 2018. 1, 2
- [43] Zhongdao Wang, Jingwei Zhang, Liang Zheng, Yixuan Liu, Yifan Sun, Yali Li, and Shengjin Wang. Cycas: Self-supervised cycle association for learning re-identifiable descriptions. *arXiv preprint arXiv:2007.07577*, 2020. 6
- [44] Longhui Wei, Shiliang Zhang, Wen Gao, and Qi Tian. Person transfer gan to bridge domain gap for person re-identification. In *Proceedings of the IEEE conference on computer vision and pattern recognition*, pages 79–88, 2018. 1, 2, 5, 7
- [45] Jinlin Wu, Yang Yang, Hao Liu, Shengcai Liao, Zhen Lei, and Stan Z Li. Unsupervised graph association for person re-identification. In *Proceedings of the IEEE/CVF International Conference on Computer Vision*, pages 8321–8330, 2019. 6
- [46] Zhirong Wu, Yuanjun Xiong, Stella X Yu, and Dahua Lin. Unsupervised feature learning via non-parametric instance discrimination. In *Proceedings of the IEEE Conference on Computer Vision and Pattern Recognition*, pages 3733–3742, 2018. 2
- [47] Tong Xiao, Shuang Li, Bochao Wang, Liang Lin, and Xiaogang Wang. Joint detection and identification feature learning for person search. In *Proceedings of the IEEE Conference on Computer Vision and Pattern Recognition (CVPR)*, July 2017. 2
- [48] Tong Xiao, Shuang Li, Bochao Wang, Liang Lin, and Xiaogang Wang. Joint detection and identification feature learning for person search. In *Proceedings of the IEEE Conference on Computer Vision and Pattern Recognition*, pages 3415–3424, 2017. 6
- [49] Hong-Xing Yu, Wei-Shi Zheng, Ancong Wu, Xiaowei Guo, Shaogang Gong, and Jian-Huang Lai. Unsupervised person re-identification by soft multilabel learning. In *Proceedings of the IEEE/CVF Conference on Computer Vision and Pattern Recognition*, pages 2148–2157, 2019. 1, 2
- [50] Kaiwei Zeng, Munan Ning, Yaohua Wang, and Yang Guo. Hierarchical clustering with hard-batch triplet loss for person re-identification. In *Proceedings of the IEEE/CVF Conference on Computer Vision and Pattern Recognition*, pages 13657–13665, 2020. 6
- [51] Yunpeng Zhai, Shijian Lu, Qixiang Ye, Xuebo Shan, Jie Chen, Rongrong Ji, and Yonghong Tian. Ad-cluster: Augmented discriminative clustering for domain adaptive person re-identification. In *Proceedings of the IEEE/CVF Conference on Computer Vision and Pattern Recognition*, pages 9021–9030, 2020. 6
- [52] Zhizheng Zhang, Cuiling Lan, Wenjun Zeng, and Zhibo Chen. Densely semantically aligned person re-identification.

- In *Proceedings of the IEEE/CVF Conference on Computer Vision and Pattern Recognition*, pages 667–676, 2019. [2](#)
- [53] Liang Zheng, Liyue Shen, Lu Tian, Shengjin Wang, Jingdong Wang, and Qi Tian. Scalable person re-identification: A benchmark. In *Proceedings of the IEEE international conference on computer vision*, pages 1116–1124, 2015. [5](#), [7](#)
- [54] Zhun Zhong, Liang Zheng, Guoliang Kang, Shaozi Li, and Yi Yang. Random erasing data augmentation. In *Proceedings of the AAAI Conference on Artificial Intelligence*, volume 34, pages 13001–13008, 2020. [7](#)
- [55] Zhun Zhong, Liang Zheng, Shaozi Li, and Yi Yang. Generalizing a person retrieval model hetero-and homogeneously. In *Proceedings of the European Conference on Computer Vision (ECCV)*, pages 172–188, 2018. [1](#), [2](#)
- [56] Zhun Zhong, Liang Zheng, Zhiming Luo, Shaozi Li, and Yi Yang. Invariance matters: Exemplar memory for domain adaptive person re-identification. In *Proceedings of the IEEE/CVF Conference on Computer Vision and Pattern Recognition*, pages 598–607, 2019. [1](#), [2](#), [6](#)
- [57] Sanping Zhou, Fei Wang, Zeyi Huang, and Jinjun Wang. Discriminative feature learning with consistent attention regularization for person re-identification. In *Proceedings of the IEEE/CVF International Conference on Computer Vision*, pages 8040–8049, 2019. [2](#)
- [58] Chengxu Zhuang, Alex Lin Zhai, and Daniel Yamins. Local aggregation for unsupervised learning of visual embeddings. In *Proceedings of the IEEE/CVF International Conference on Computer Vision*, pages 6002–6012, 2019. [2](#)